ELSEVIER

Ceramics International 31 (2005) 39–46

CERAMICS INTERNATIONAL

www.elsevier.com/locate/ceramint

Mechanical behavior of zirconia/alumina composites

S.R. Choi*, N.P. Bansal

NASA Glenn Research Center, Cleveland, OH 44135, USA

Received 29 October 2003; received in revised form 16 January 2004; accepted 1 March 2004
Available online 26 June 2004

Abstract

Zirconia/alumina composites were fabricated by hot pressing 10 mol% yttria-stabilized zirconia (10-YSZ) reinforced with 0–30 mol% alumina particulates or platelets. Flexure strength and fracture toughness of both particulate and platelet composites increased with increasing alumina content. For a given alumina content, strength of particulate composites was greater than that of platelet composites; whereas, difference in fracture toughness between the two composite systems was negligible. No difference in elastic modulus and density was observed for a given alumina content between particulate and platelet composites. Thermal cycling up to 10 cycles between 200 and 1000 °C did not show any strength degradation of the 30 mol% platelet composites, indicative of negligible influence of coefficient-of-thermal-expansion mismatch between YSZ and alumina grains.

Keywords: B. Composites; C. Mechanical properties; C. Strength; C. Hardness; D. Al_2O_3; D. ZrO_2

1. Introduction

Yttria-stabilized zirconia (YSZ) is the most commonly used electrolyte in solid oxide fuel cell (SOFC) because of its high oxygen ion conductivity, stability in both oxidizing and reducing environments, availability, and low cost [1]. However, similar to other ceramics, YSZ is brittle and susceptible to fracture due to the existence of flaws, which are introduced during fabrication and use of the SOFC. In addition, the properties of YSZ such as low thermal conductivity and relatively high thermal-expansion coefficient make this material thermal-shock sensitive. Fracture in the solid oxide electrolyte will allow the fuel and oxidant to come in contact with each other resulting in reduced cell efficiency or in some cases malfunction of the SOFC. Therefore, YSZ solid electrolyte with high fracture toughness as well as enhanced strength is required for good performance and structural reliability.

The objective of this study was to improve the strength and fracture toughness of 10 mol% yttria-stabilized zirconia (10-YSZ) by reinforcing with 0–30 mol% alumina particulates or platelets without degrading ionic conductivity to an appreciable extent. Strength, fracture toughness, and other properties such as elastic modulus, density and microhardness of YSZ/alumina composites were determined as a function of alumina content. The effect of residual stresses and/or microcracking, due to coefficient of thermal expansion (CTE) mismatches between YSZ matrix and alumina grains, was also examined by thermal cycling experiment.

2. Experimental procedures

2.1. Processing and microstructural characterization

Material processing has been described in detail elsewhere [2,3]. Briefly, the starting materials used were 10-mol% yttria fully stabilized zirconia powder (HSY-10, average particle size 0.41 μm, specific surface area 5.0 m^2/g) from Daiichi Kigenso Kagaku Kogyo Co., Japan, alumina powder (high purity BAILALOX CR-30, 99.99% purity, average particle size 0.05 μm, specific area 25 m^2/g) from Baikowski International Corporation, Charlotte, NC, USA, and alpha alumina hexagonal platelets (Pyrofine Plat Grade T2, average aspect ratio 10–15, average length 10–15 μm) from Elf Atochem, France. Appropriate quantities of alumina and zirconia powders were slurry mixed in acetone and mixed for ∼24 h using zirconia media. Acetone was then evaporated and the

* Corresponding author at Ohio Aerospace Institute.
Tel.: +1-216-433-8366; fax: +1-216-433-8300.
E-mail address: sung.r.choi@grc.nasa.gov (S.R. Choi).

0272-8842/$30.00 © 2004 Elsevier Ltd and Techna S.r.l. All rights reserved.
doi:10.1016/j.ceramint.2004.03.032

powder dried in an electric oven. The resulting powder was loaded into a graphite die and hot pressed at 1500 °C in vacuum under 30 MPa pressure into 152 mm × 152 mm billets using a hot press. Grafoil was used as spacers between the specimen and the punches. Various hot pressing cycles were tried in order to optimize the hot pressing parameters that would result in dense and crack free ceramic samples [3]. YSZ/alumina composites containing 0, 5, 10, 20, and 30 mol% alumina were fabricated for each particulate and platelet composite systems.

The billets were machined into flexure bar test specimens with nominal depth, width and length of 3.0 mm × 4.0 mm × 50 mm, respectively, in accordance with ASTM test standard C 1161 [4]. Machining direction was longitudinal along the 50 mm-length direction. It should be noted that unlike transformation-toughened (from tetragonal to monoclinic) zirconias, the cubic yttria-stabilized zirconia is very unlikely to induce any transformation-associated residual stresses on the surfaces of test specimens due to machining. The sharp edges of test specimens were chamfered to reduce any spurious premature failure emanating from those sharp edges.

X-ray diffraction (XRD) pattern were recorded using a step scan procedure (0.02°/2θ, time per step 0.5 or 1 s) on a Philips ADP-3600 automated diffractometer equipped with a crystal monochromator employing Cu Kα radiation. Microstructures of the polished surfaces were observed in a JEOL JSM-840A scanning electron microscope (SEM). Thin foils for transmission electron microscopy (TEM) were prepared using a procedure that involved slicing, polishing, and argon ion beam milling. The thin foils were examined in a Philips EM-400T operating 120 keV. A thin carbon coating was evaporated onto the TEM thin foils. X-ray element analyses of the phases were carried out using a Kevex Delta thin window energy dispersive spectrometer (EDS) and analyzer.

2.2. Flexure strength and fracture toughness testing

All strength testing was carried out in flexure at ambient temperature in air. A four-point flexure fixture with 20 mm-inner and 40 mm-outer spans was used in conjunction with an electromechanical test frame (Model 8562, Instron, Canton, MA, USA). A fast stress rate of 50 MPa/s was applied in load control using the test frame to reduce slow crack growth effect of the materials. A total of 10 test specimens were tested for each composite. All tests were conducted in accordance with ASTM test standards C1161 [4].

Fracture toughness using flexure bar specimens measuring 3 mm × 4 mm × 25 mm or 50 mm was determined at ambient temperature in air using single edge v-notched beam (SEVNB) method [2,5]. This method utilizes a razor blade with diamond paste, grain size of 9 μm, to introduce a final sharp notch with a root radius ranging 10–20 μm by tapering a saw notch. The sharp v-notched specimens with a notch depth of 0.9 mm were fractured in a four-point flexure fixture with 20 mm-inner and 40 mm-outer spans using the electromechanical test frame at an actuator speed of 0.5 mm/min. Five specimens were tested for each composite. Fracture toughness (K_{Ic}) was calculated based on the formula by Srawley and Gross [6] as follows:

$$K_{Ic} = \frac{P_f(L_o - L_i)}{BW^{3/2}} \frac{3\alpha^{1/2}}{2(1-\alpha)^{3/2}} f(\alpha)$$

where P_f, L_o, L_i, B, W are fracture load, outer span, inner span, specimen width, and specimen depth, respectively, $\alpha = a/W$ with a being precrack size, and $f(\alpha)$ is expressed as:

$$f(\alpha) = 1.9887 - 1.326\alpha - \frac{\alpha(1-\alpha)(3.49 - 0.68\alpha + 1.35\alpha^2)}{(1+\alpha)^2}$$

2.3. Elastic modulus, density, and microhardness

Elastic modulus was determined at ambient temperature by the impulse excitation of vibration method, ASTM C 1259 [7], using the flexure specimen configuration. Density was measured with a bulk mass/volume method using the same flexure specimens that were used in elastic modulus experiment. Five specimens of each composite were used for elastic modulus as well as in density measurements. Microhardness of the composites was evaluated at ambient temperature with a Vickers microhardness indenter with an indent load of 9.8 N using five indents for each composite, in accordance with ASTM C 1327 [8].

2.4. Thermal cycling testing

Thermal cycling (fatigue) test was carried out for the 10-YSZ/30 mol% platelet alumina by applying a total of 10 thermal cycles of heating (1000 °C) and cooling (200 °C) in air using five flexure specimens. The rate of heating and cooling was about 10 and 20 °C/min, respectively. These specimens were then fractured at ambient temperature in four-point flexure to determine their corresponding flexure strength. This testing was conducted to better understand the effect of CTE mismatches on flexure strength, possibly resulting in strength degradation due to residual stresses and/or microcracks induced by CTE mismatches between YSZ matrix and alumina grains.

3. Results and discussion

3.1. Microstructural characterization

Scanning electron microscopy from polished cross-sections of YSZ/alumina composites showed that alumina particulates [2] as well as alumina platelets were reasonably well dispersed throughout YSZ matrix but some conglomeration was inevitable. Typical micrographs for polished surfaces—planes perpendicular to hot pressing direction—of 20 mol% particulate and platelet composites

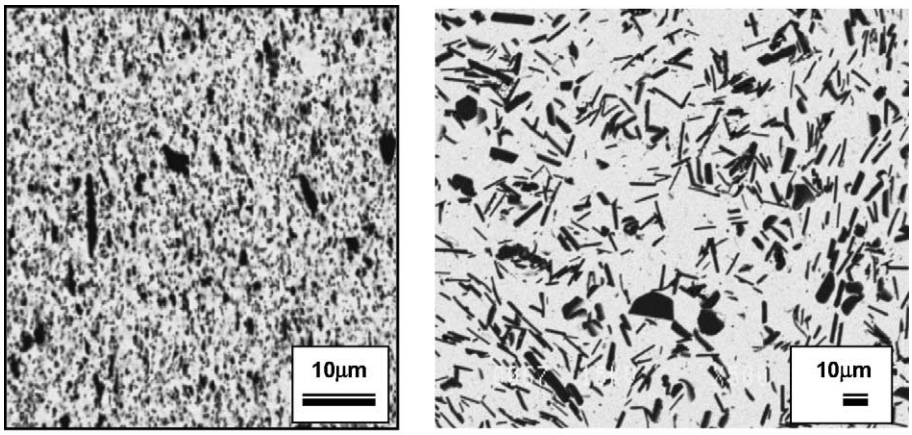

Fig. 1. SEM micrographs showing polished surfaces (normal to hot-pressing direction) of 10-YSZ/20 mol% alumina particulate and platelet composites: (a) particulate; (b) platelet.

are shown in Fig. 1. The dark areas represent alumina particulates or platelets while the light areas indicate the 10-YSZ matrix, as analyzed via SEM/EDS. Pores were also visible as dark objects. Bulk density of both particulate and platelet composites and 10-YSZ was in the range of 98–99% of theoretical density. Results of X-ray diffraction analysis for both composites showed phases of cubic YSZ and α-alumina. TEM micrographs and X-ray elemental maps indicated that an average, equiaxed grain size was about less than 1.0 μm for YSZ matrix, as shown in Fig. 2. Figs. 3 and 4 indicate that grain boundaries and triple junctions exhibited little presence of amorphous phase for both 0 and 30 mol% particulate composites. No appreciable deformation or microcracks of adjacent grains that might occur due to thermoelastic mismatches between YSZ matrix and alumina were observed in the particulate composites from a TEM micrograph analysis [2,3].

3.2. Flexure strength

The results of strength testing for both particulate and platelet composites are shown in Fig. 5. Strength of the particulate composites increased with increasing alumina content, while strength of the platelet composites remained almost unchanged with increasing alumina content, except at 5 mol%. Hence, increase in strength was much more significant in the particulate composites than in the platelet composites. For a given alumina content, strength of particulate composites was 15–30% greater than that of platelet composites. Strength of the 30 mol% particulate composite was 40% greater than the 10-YSZ (matrix) strength. The 10-YSZ strength ($= 280 \pm 23$ MPa) was in reasonable agreement with the strength value (≈240–300 MPa) typically observed in 6.5 to 8-YSZ [9,10]. Weibull modulus (m), estimated despite a limited number (=10) of test specimens, was in the range of 5–15, a little greater for the platelet composites than for the particulate composites: $m = 13 \pm 4$, 7 ± 2, and 11 for the platelet, particulate, and 10-YSZ, respectively. Fracture originated from surface defects, associated with pores and machining damage in many cases. Overall flaw sizes, ranging from 20 to 60 μm, were greater for the platelet composites than for the particulate counterparts. Typical examples of fracture surfaces of specimens showing surface-flaw-associated failure for both 30 mol% particulate and platelets composites are shown in Fig. 6.

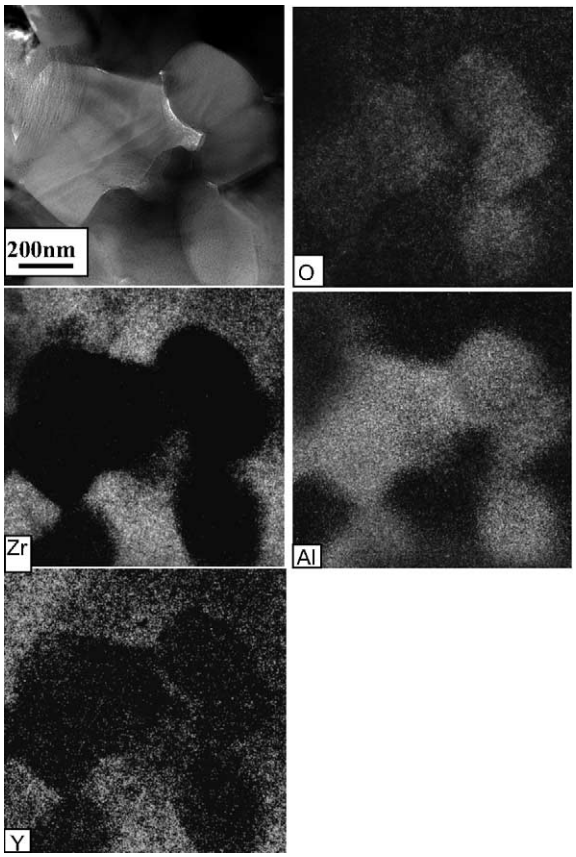

Fig. 2. TEM micrograph showing zirconia and alumina grains and X-ray element maps of different elements for 10-YSZ/alumina particulate composite containing 30 mol% alumina.

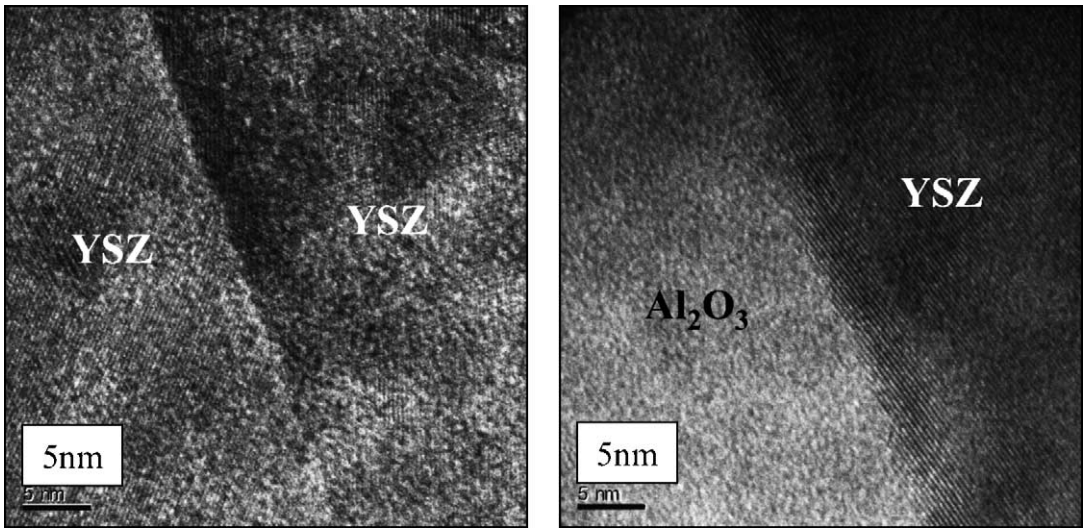

Fig. 3. TEM micrographs showing grain boundaries in 10-YSZ/alumina particulate composites containing: (a) 0 mol% alumina; (b) 30 mol% alumina.

Some other zirconia/alumina composites exhibited a strength decrease with increasing alumina content, in part as a result of internal (tensile) residual stresses by the CTE mismatch between zirconia matrix and alumina particulate (or platelets) [11,12]. By contrast, fracture toughness is known to increase due to more enhanced crack deflection/bridging [13]. Based on the results of strength increase with increasing alumina content as seen in Fig. 5, it can be stated that the alumina particulates or platelets used in this work might not have interacted with the matrix to produce residual stresses by CTE mismatches sufficient enough to degrade composite strength. This issue of CTE mismatches on strength degradation will be discussed with the result of thermal cycle testing in Section 3.5. The reason why the particulate composites exhibited more improved strength than the platelet composites is probably due to the fact that alumina particulates might have acted as more reinforcing

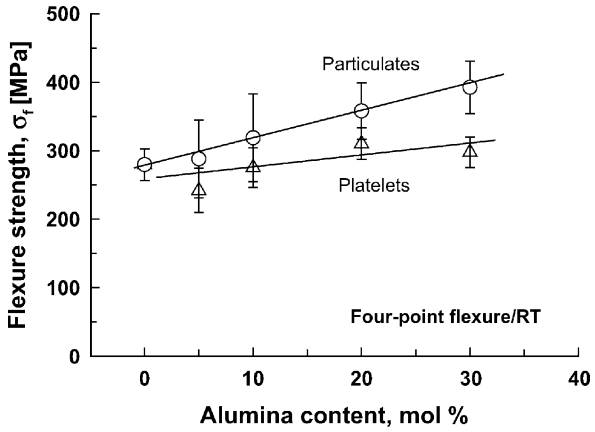

Fig. 5. Flexure strength of 10-YSZ/alumina particulate and platelet composites as a function of alumina content at ambient temperature in air. Error bars indicate ±1.0 standard deviation. The lines represent the best fit.

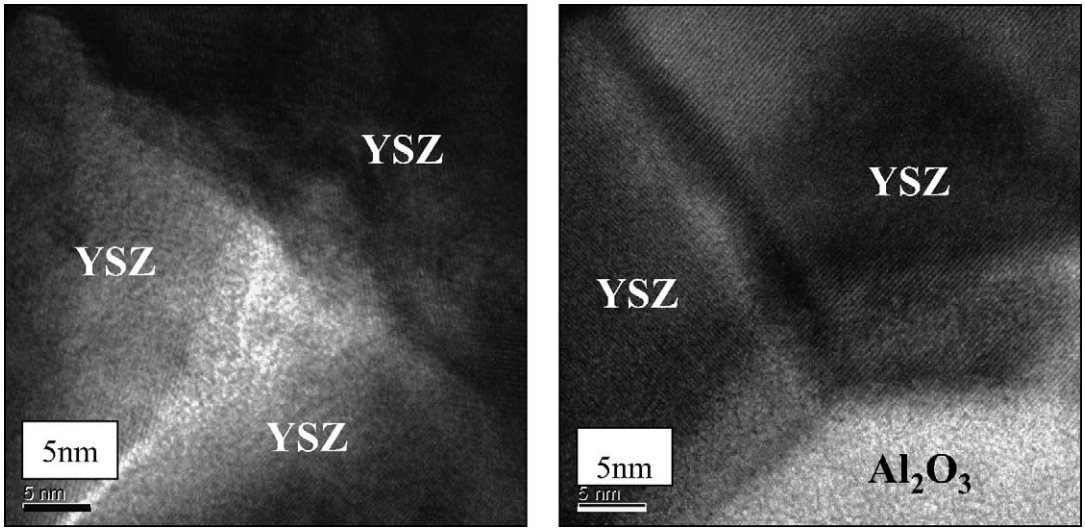

Fig. 4. TEM micrographs showing triple junctions in 10-YSZ/alumina particulate composites containing: (a) 0 mol% alumina; (b) 30 mol% alumina.

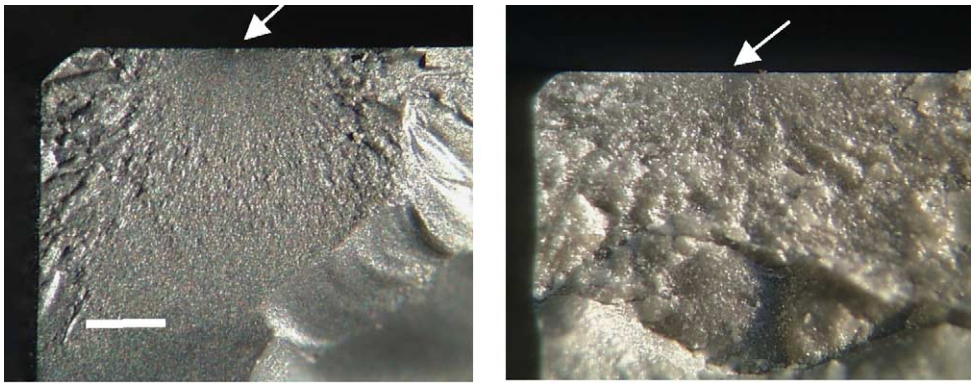

Fig. 6. Typical examples of overall fracture surfaces showing fracture origins with arrows for: (a) 10-YSZ/30 mol% alumina particulate composite; (b) 10-YSZ/30 mol% alumina platelet composite. Bar = 500 μm.

medium than strength-controlling flaws, while alumina platelets might have acted as less reinforcing medium, typical of many platelets-reinforced composites.

3.3. Fracture toughness

A summary of the results of fracture toughness testing is presented in Fig. 7, in which fracture toughness determined by the SEVNB method was plotted as a function of alumina mol% for both particulate and platelet composites. Similar to the trend in flexure strength, fracture toughness increased with increasing alumina content. Fracture toughness increased by 65 and 62%, respectively, for the particulate and platelet composites when alumina content increased from 0 to 30 mol%. Fracture toughness ($=1.6 \pm 0.1\,\mathrm{MPa\,m^{1/2}}$) of 10-YSZ was in line with a general trend as exhibited by other fully stabilized zirconias with >8 mol% yttria, in which fracture toughness ranged from 1 to $2\,\mathrm{MPa\,m^{1/2}}$ [14,15]. It is noted that unlike the flexure strength the difference in fracture toughness between the particulate and platelet composites was negligible. It has been observed that an incompatibility is generally operative for many composites between strength and fracture toughness such that one property increases while the other decreases. However, this was not the case for the current two composite systems, resulting in not only strength increase (particularly for the particulate composites) but also fracture-toughness increase with increasing alumina content.

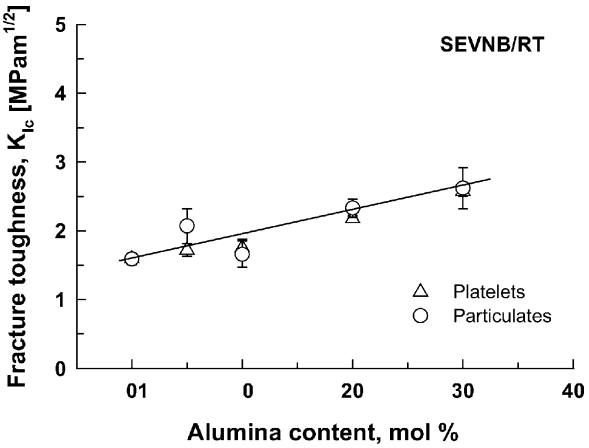

Fig. 7. Fracture toughness of as a function of alumina content for both 10-YSZ/alumina particulate and platelet composites, determined by the SEVNB method at ambient temperature. Error bars indicate ±1.0 standard deviation.

Although not presented here, it was observed that indent crack trajectories of both 0 and 30 mol% composites were characterized such that the straight path and greater COD (crack opening displacement) of a crack was typified for 10-YSZ (0 mol% composite); whereas, the tortuous path around alumina grains and less COD was exemplified for the 30 mol% particulate or platelet composite. More enhanced crack interactions with alumina grains with increasing alumina content is thus believed to be responsible for the increased fracture toughness for both composite systems. A notion that platelets would be more efficient in enhancing fracture toughness than particulates was not applicable in these composite systems. Note that the cubic 10-YSZ is not a stress-induced, transformation toughened ceramic. Therefore, the increased fracture toughness with increasing alumina content would be a logical reasoning for the increase in flexure strength observed from the two composite systems, since flaw sizes of either particulate or platelet composites appeared to be not much different, regardless of alumina content.

3.4. Elastic modulus, density, and microhardness

The results of elastic modulus, density and microhardness measurements are presented in Fig. 8. Elastic modulus increased linearly with increasing alumina content for both particulate and platelet composites, resulting in little difference in elastic modulus between the two composite systems. The 10-YSZ agreed well in elastic modulus

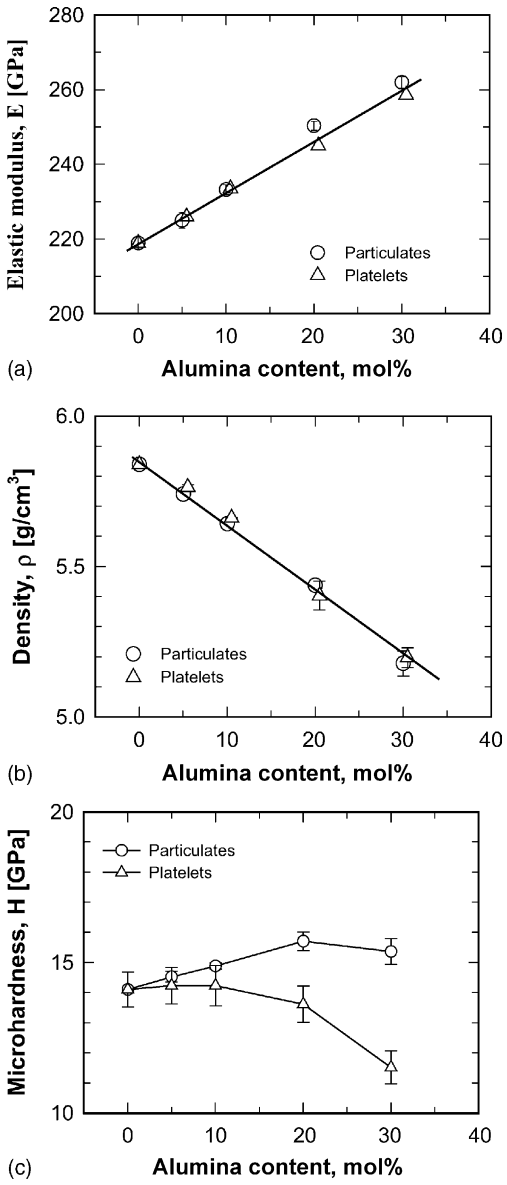

Fig. 8. (a) Elastic modulus determined by impulse excitation [7], (b) density, and (c) Vickers microhardness [8], as a function of alumina content for 10-YSZ/alumina particulate and platelet composites at ambient temperature as a function of alumina content. Error bars indicate ±1.0 standard deviation. The line in elastic modulus indicates the prediction based on the rule of mixture.

($E = 219 \pm 2$ GPa) with other zirconias such as 6.5-YSZ, 8-YSZ, Y-PSZ, Y-TZP, and Mg-PSZ [9,16,17] whose elastic modulus ranged commonly between 200 and 220 GPa. The prediction based on the rule of mixture was in good agreement with the experimental data as shown in the figure. Values of $E_{10\text{-YSZ}} = 220$ GPa and $E_{\text{Alumina}} = 370$ GPa were used in the prediction. Density (ρ) decreased linearly with increasing alumina content for both composite systems, yielding negligible difference within the scatter for a given alumina content between the two composites. Note that this bulk density ranged from 98 to 99% of theoretical density

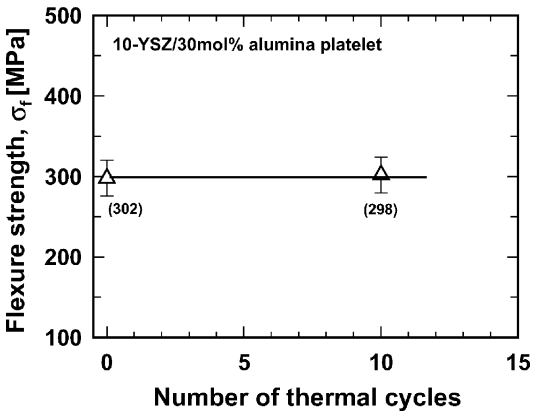

Fig. 9. Flexure strength as a function of number of thermal cycles (between 200 and 1000 °C) for 10-YSZ/30 mol% alumina platelet composite. The numbers in parentheses indicate average strength. Error bars indicate ±1.0 standard deviation.

for either particulate or platelet or 10-YSZ, as mentioned in Section 3.1.

Microhardness increased linearly with increasing alumina content for the particulate composites up to 20 mol% alumina and then leveled up above 20 mol%. By contrast, microhardness of the platelet composites remained almost unchanged up to 10 mol% and then decreased appreciably at 30 mol%, resulting in a significant difference in hardness at 30 mol% between the two composites. The reason for the unique decrease in microhardness for the platelet composite above 20 mol% is not known yet.

3.5. Thermal fatigue

The result of thermal cycling (fatigue) test for the 30 mol% platelet composite is shown in Fig. 9. There was no difference in strength between 0 (regular strength test) and 10 thermal cycles, indicating that repeated thermal cycling up to 10-times did not show any significant effect on strength degradation for the composite under the test condition used. In other words, internal residual stresses and/or microcracks due to CTE mismatches between zirconia matrix and alumina grains possibly occurring in thermal fatigue were negligible to affect flexure strength of the composite material of interest. Hence, it is concluded that CTE mismatch would not have been operative sufficient enough to degrade strength of the composite systems.

3.6. Choice of material with respect to structural reliability and SOFC performance

As seen in the foregoing results, both flexure strength and fracture toughness increased with increasing alumina content. For a given alumina content, flexure strength of the particulate composites was greater than that of the platelet composites, while fracture toughness of both composite systems remained almost identical. Elastic modulus increased

with increasing alumina, and density decreased with increasing alumina content. Therefore, from a structural reliability point of view, a composite which is strongest (in strength), toughest (in fracture toughness), stiffest (in elastic modulus) and lightest (in weight) is certainly the best choice, which undoubtedly leads to the 30 mol% particulate composite. This structural consideration, however, should not neglect the SOFC's important electrical performance, oxygen (O^{2-})-ion conductivity. Although not presented here, a preliminary study on ionic conductivity of both particulate and platelet composites showed that ionic conductivity was not appreciably dependent on alumina content particularly at higher temperatures of 1000 and 1100 °C. This is contrary to a notion that addition of non-conducting alumina to 10-YSZ, especially with 30 mol% alumina, can lower ionic conductivity. However, Oe et al. [18] also showed that ionic conductivity of 8-YSZ remained almost comparable up to 1000 °C with that of 8-YSZ reinforced with 30 mol% alumina, reasoning that alumina particles might have been dispersed randomly in matrix grains rather than segregated at grain boundaries.

It is also expected that both composite systems would exhibit time-dependent behavior such as slow crack growth or fatigue at elevated temperatures, since in particular alumina has shown enhanced slow crack growth behavior at elevated temperatures >700 °C in air [19]. As a consequence, the determination of life prediction parameters of chosen YSZ/alumina composites at elevated temperatures, close to typical SOFCs operating temperature around 1000 °C, is a prerequisite to ensure accurate life/reliability of fuel cell components fabricated with zirconia/alumina composites. The results of life prediction parameters study will be reported elsewhere.

4. Conclusions

1. The flexure strength and fracture toughness of 10-mol% yttria-stabilized zirconia reinforced with 0–30 mol% alumina particulates or platelets were determined as a function of alumina content at ambient temperature in air. Both flexure strength and fracture toughness increased with increasing alumina content. For a given alumina content, strength of particulate composites was greater than that of platelet composites, while the difference in fracture toughness between the two composite systems was insignificant.
2. Difference in elastic modulus and density was negligible for a given alumina content between the particulate and platelet composites. By contrast, microhardness was greater for the particulate composites than for the platelet counterparts, particularly above 20 mol% alumina contents.
3. Thermal cycling up to 10 cycles between 200 and 1000 °C did not show any adverse effect on strength degradation of the 30 mol% platelet composites, indicative of negligible influence of CTE mismatch between YSZ matrix and alumina grains.

Acknowledgements

The authors are grateful to Ralph Pawlik for mechanical testing and John Setlock for materials processing. This work was supported by Zero CO_2 Emission Technology (ZCET) Project of the Aerospace Propulsion and Power Program, NASA Glenn Research Center, Cleveland, OH.

References

[1] N.Q. Minh, Ceramic fuel cells, J. Am. Ceram. Soc. 76 (3) (1993) 563–588.
[2] S.R. Choi, N.P. Bansal, Strength and fracture toughness of zirconia/alumina composites for solid oxide fuel cells, Ceram. Eng. Sci. Proc. 23 (3) (2002) 741–750.
[3] N.P. Bansal, S.R. Choi, Processing of Alumina-Toughened Zirconia Composites, NASA/TM-2003-212451, National Aeronautics and Space Administration, Glenn Research Center, Cleveland, OH, 2003.
[4] ASTM C 1161, Test method for flexural strength of advanced ceramics at ambient temperature, in: Annual Book of ASTM Standards, vol. 15.01, American Society for Testing and Materials, West Conshohocken, PA, 2003.
[5] (a) J. Kübler, Fracture toughness of ceramics using the SEVNB method: preliminary results, Ceram. Eng. Sci. Proc. 18 (4) (1997) 155–162;
(b) Fracture toughness of ceramics using the SEVNB method, round robin, in: VAMAS Report No. 37, EMPA, Swiss Federal Laboratories for Materials Testing and Research, Dübendorf, Switzerland, 1999.
[6] J.E. Srawley, B. Gross, Side-cracked plates subjected to combined direct and bending forces, in: Cracks and Fracture, ASTM STP 601, American Society for Testing and Materials, Philadelphia, 1976, pp. 559–579.
[7] ASTM C 1259, Test method for dynamic Young's modulus, shear modulus, and Poisson's ratio for advanced ceramics by impulse excitation of vibration, in: Annual Book of ASTM Standards, vol. 15.01, American Society for Testing and Materials, West Conshohocken, PA, 2003.
[8] ASTM C 1327, Test method for Vickers indentation hardness of advanced ceramics, in: Annual Book of ASTM Standards, vol. 15.01, American Society for Testing and Materials, West Conshohocken, PA, 2001.
[9] J.W. Adams, R. Ruh, K.S. Mazdiyasni, Young's modulus, flexural strength, and fracture of yttria-stabilized zirconia versus temperature, J. Am. Ceram. Soc. 80 (4) (1997) 903–908.
[10] A. Kishimoto, M. Ito, S. Fujitsu, Microwave sintering of ion conductive zirconia based composite dispersed with alumina, J. Mater. Sci. Lett. 20 (2001) 943–945.
[11] F.F. Lange, Transformation toughening, Part 4. Fabrication, J. Mater. Sci. 17 (1982) 247–254.
[12] I.K. Cherian, W.M. Kriven, Alumina-platelet-reinforced 3Y-TZP, Am. Ceram. Soc. Bull. 80 (12) (2001) 57–63.
[13] K.T. Faber, A.G. Evans, Crack deflection processes, Acta. Metall. 31 (4) (1983) 565–576.
[14] F.F. Lange, Transformation toughening, Part 3. Experimental observations in the ZrO_2–Y_2O_3 system, J. Mater. Sci. 17 (1982) 240–256.
[15] T. Sakuma, Y.-I. Yoshizawa, H. Suto, The microstructure and mechanical properties of yttria-stabilized zirconia prepared by arc-melting, J. Mater. Sci. 20 (1985) 2399–2407.

[16] M. Shimada, K. Matsushita, S. Kuratani, T. Okamoto, K. Tsukuma, T. Tsukidate, Temperature dependence of Young's modulus and internal friction in alumina, silicon nitride, and partially stabilized zirconia ceramics, J. Am. Ceram. Soc. 67 (2) (1984) C23–C24.
[17] D.C. Larson, J.W. Adams, Long-term Stability and Properties of Zirconia Ceramics for Heavy Duty Diesel Engine Components, NASA CR-174943, Washington, DC, 1985.
[18] K. Oe, K. Kikkawa, A. Kishimoto, Y. Nakamura, H. Yanagida, Toughening of ionic conductive zirconia ceramics utilizing a non-linear effect, Solid State Ionics 91 (1996) 131–136.
[19] S.R. Choi, J.P. Gyekenyesi, Elevated-temperature 'ultra'-fast fracture strength of advanced ceramics: an approach to elevated-temperature 'inert' strength, ASME J. Eng. Gas Turbines Powers 121 (1999) 18–24.